RESEARCH ARTICLE

Macromolecular Bioscience

www.mbs-journal.de

Characterization of Tunable Poly-ϵ-Lysine-Based Hydrogels for Corneal Tissue Engineering

*Rebecca Lace, Georgia L. Duffy, Andrew G. Gallagher, Kyle G. Doherty, Osama Maklad, Donald A. Wellings, and Rachel L. Williams**

A family of poly-ϵ-lysine hydrogels can be synthesized by crosslinking with bis-carboxylic acids using carbodiimide chemistry. In addition to creating hydrogels using a simple cast method, a fragmented method is used to introduce increased porosity within the hydrogel structure. Both methods have created tunable characteristics ranging in their mechanical properties, transparency, and water content, which is of interest to corneal tissue engineering and can be tailored to specific cellular needs and applications. With a worldwide shortage of cornea donor tissue available for transplant and limitations including rejection and potential infection, a synthetic material that can be used as a graft, or a partial thickness corneal replacement, would be an advantageous treatment method. These hydrogels can be tuned to have similar mechanical and transparency properties to the human cornea. They also support the attachment and growth of corneal epithelial cells and the integration of corneal stromal cells.

1. Introduction

The cornea is the transparent window at the front of the eye. It helps to focus light onto the retina and also functions as a barrier to protect the eye against UV radiation and the invasion of particles.[1] It is made up of three main layers, a stratified epithelium, the stroma, and the endothelium. The current treatment for damage to any of these layers is either a partial or full thickness corneal transplant from a cadaveric donor.[2] However, there is a shortage of donor cornea tissue available for transplantation, with over 10 million people currently on the waiting list worldwide.[3] Additional limitations of this procedure include potential tissue rejection, infection, and the high overall expense.[4] These limitations have pushed research toward biomaterials and tissue engineering methods to introduce suitable alternative treatments.

Tissue engineering approaches to corneal regeneration have been widely investigated. Various natural and synthetic substrates have been evaluated as both scaffolds for stromal implantation and cell delivery vehicles for the epithelial and endothelial layers, and have their own advantages and disadvantages. Amniotic membrane has been used clinically for ocular surface reconstruction of the epithelium and for limbal stem cell transplantation,[5] however the use of donor tissue presents a risk of disease transmission and difficulties with donor tissue variability. Silk fibroin has been manufactured into membranes, which have demonstrated a high transparency and supported the culture of stromal and epithelial cells in vitro,[6] however when compared to alternative hydrogels for corneal tissue engineering, have demonstrated brittle mechanical properties. Synthetic polymers such as poly(lactide-*co*-glycolide) (PLGA) can be electrospun into scaffolds that have been shown to support epithelial stem cell expansion,[7] however, when these structures were used in early clinical trials, they were found to be too stiff for clinical use. Overall, due to the corneas complex structure, few full thickness corneal replacements have made it through to clinical trials.[8]

The use of hydrogels based on peptides has emerged into the field of tissue engineering due to the versatility of material fabrication and the desirable material properties. Peptides can be manufactured into a variety of structures, such as those that mimic the extracellular matrix (ECM).[9] 3D peptide hydrogels

Dr R. Lace, G. L. Duffy, Dr. K. G. Doherty, Prof. R. L. Williams
Department of Eye and Vision Science
Institute of Life Course and Medical Science
University of Liverpool
Liverpool L7 8TX, UK
E-mail: rlw@liverpool.ac.uk
Dr. A. G. Gallagher[+], Dr. D. A. Wellings
SpheriTech Ltd.
Business and Technical Park
The Heath
Runcorn WA7 4QX, UK
Dr. O. Maklad[++]
School of Engineering
University of Liverpool
Brownlow Hill, Liverpool L69 3GH, UK

The ORCID identification number(s) for the author(s) of this article can be found under https://doi.org/10.1002/mabi.202100036

[+]Present address: CÚRAM, SFI Research Centre for Medical Devices, Biomedical Sciences, National University of Ireland Galway, Galway H91 W2TY, Ireland

[++]Present address: School of Engineering, Liverpool John Moores University, Liverpool L3 3AF UK

DOI: 10.1002/mabi.202100036

in particular have been intensively researched due to their high porosity, mechanical stability, hydrophilicity, and biomimetic tunability.[10] Additionally, hydrogels maintain a high water content, therefore are able to mimic the 78% water content of the cornea.[11] Cell adhesion to hydrogels can be further encouraged with the addition of peptides containing the arginylglycylaspartic acid (RGD) sequence and laminins. These can be easily bound to the peptide hydrogels due to the presence of amine and carboxyl functional groups in the polymer chains. Peptides are suitable for biomaterial applications as they act as molecular building blocks, which are biocompatible, easily synthesized, and have been thoroughly investigated.[12] Self-assembling peptide hydrogels are synthesized based on their ability to form various covalent and noncovalent interactions, such as hydrogen bonds, hydrophobic force, and electrostatic interaction.[13] These various interactions allow peptide hydrogels to have stimuli responsive properties, encouraging polymerization to occur based on a change in temperature, pH, electric field, or chemical reaction. Stimuli-responsive hydrogels have found bioapplications in bioimaging, targeted drug delivery, and biosensors.[14]

However, self-assembling peptide hydrogels demonstrate inferior mechanical properties due to these electrostatic interactions when compared to hydrogels made using the peptide at the focus of this study, poly-ε-lysine (pεK). This is a naturally occurring homo-poly-amide of L-lysine, which is water soluble, nontoxic, biodegradable, and thermostable.[15] Additionally, crosslinking pεK with diacids allows for ease of producing large volumes when compared to self-assembling peptide hydrogels. Hydrogels based on this peptide have a high water content and transparency, tunable mechanical properties, and the capability for the attachment of biomolecules.[16] One limitation that substitute materials can have for corneal replacements is bacterial endophthalmitis, however within our group, we have investigated the antimicrobial benefits of pεK hydrogel's activity against Gram positive and Gram negative bacteria.[16–17] When investigated for an antimicrobial contact lens, these hydrogels did not induce any cytotoxicity in a human corneal epithelial cell line and demonstrated optical and mechanical properties comparable to commercial contact lenses.[16] In addition, pεK hydrogels encouraged the growth of corneal endothelial cells on their surface,[18] suggesting a potential application as a synthetic substrate for the replacement of damaged corneal endothelium. When combined, our previous work demonstrates that pεK is a suitable peptide for the basis of hydrogels for both corneal epithelial and endothelial tissue engineering. Further investigation into corneal stromal tissue engineering is ongoing. This study aimed to characterize a library of pεK hydrogels, which can be manufactured using alternative methods to produce cast or fragmented hydrogels suitable for different applications within corneal tissue engineering (**Figure 1**).

pεK hydrogel variants were synthesized using carbodiimide chemistry as previously described.[16,18b,19] Four bis-carboxylic acids that varied in carbon chain length were chosen for the cast pεK hydrogel variants and eight pεK hydrogel variants per bis-carboxylic acid were investigated (Table S1, Supporting Information). The mechanical and physical properties of all hydrogels were investigated. The surface topography and cell interactions on a selection of cast hydrogels were also examined. The fragmented pεK hydrogels were produced using one bis-carboxylic acid, oct-acid (Table S2, Supporting Information), and the mechanical and physical properties along with the cell interactions were studied. A summary of how the polymer chemistry and manufacture method affected the mechanical and physical properties of the hydrogels was included (Table S3, Supporting Information).

2. Results and Discussion

Throughout the literature the biomechanical properties of the human cornea have been studied, this varies from study to study due to the method of testing such as: models based on clinical examinations, uniaxial tensile strip tests, compression, or indentation methods. When investigated, all cast pεK hydrogel variants had a higher modulus in compression compared to tensile testing. For all hydrogels stiffness increased with increasing density of pεK polymer within the hydrogel, for both compression and tensile testing. Increasing the % crosslinking of the hydrogel had little effect on stiffness, especially between 60% and 90% in compressive strength (**Figure 2**A). For tensile stiffness, the % crosslinking had a greater effect on the modulus, where it was seen that 60% crosslinked hydrogel variants had the highest stiffness, across all bis-carboxylic acid variants (Figure 2B). The general trend for ultimate tensile strength (UTS) was that within each diacid and % crosslinking (for example, 60%-oct-acid) the UTS increased with increasing pεK density within the hydrogel variant (Figure S1, Supporting Information). A recent review by Palchesko et al. suggests the human cornea had a stiffness between 0.3 and 3 MPa;[20] these values cover the full range of our cast hydrogels in compression testing and the 60-0.1 and 60-0.13 pεK hydrogel variants when tensile tested. Another study based on a clinical method estimated the modulus of elasticity of the human cornea as 0.29 MPa; this is a similar value to 30-0.13 hydrogels (with the exception of dec-acid) and all 60-0.1 and 60-0.13 pεK hydrogel variants when tensile testing.[21] In addition, in comparison to commercial contact lens materials our cast hydrogels fell within a similar range to the majority.[22] These properties demonstrate handleability, and this would be important for surgical manipulation. Alternatives to native tissue corneal replacements have mainly focused on amniotic membrane and collagen derived hydrogels, however in terms of their mechanical properties and handleability these are often suboptimum.[2,5,20] Silk-derived hydrogels have also been investigated for corneal replacements and have demonstrated improved mechanical strength compared to collagen hydrogels,[23] however, they lack specific cell binding motifs and may require a feeder layer for primary cells.[2,23] Here, we have demonstrated that we can achieve mechanical properties similar to the native cornea with our cast hydrogels. In addition, our pεK hydrogel variants have previously demonstrated successful attachment of corneal endothelial cells.[18b]

For the pεK hydrogel to be a successful tissue engineering corneal replacement, in addition to the hydrogel providing mechanical stability and protection, it must be transparent and provide a scaffold, which supports specific cell organization.[24] One of the drawbacks with amniotic membrane and collagen hydrogels are their opacity.[2,5,20] The transparency of pεK hydrogel was analyzed by measuring the % light transmission (Figure 2C). All 30% crosslinked hydrogels had high transparency with a minimum light transmission of 90.2%. Increasing the density of polymer within the hydrogel did not decrease transparency.

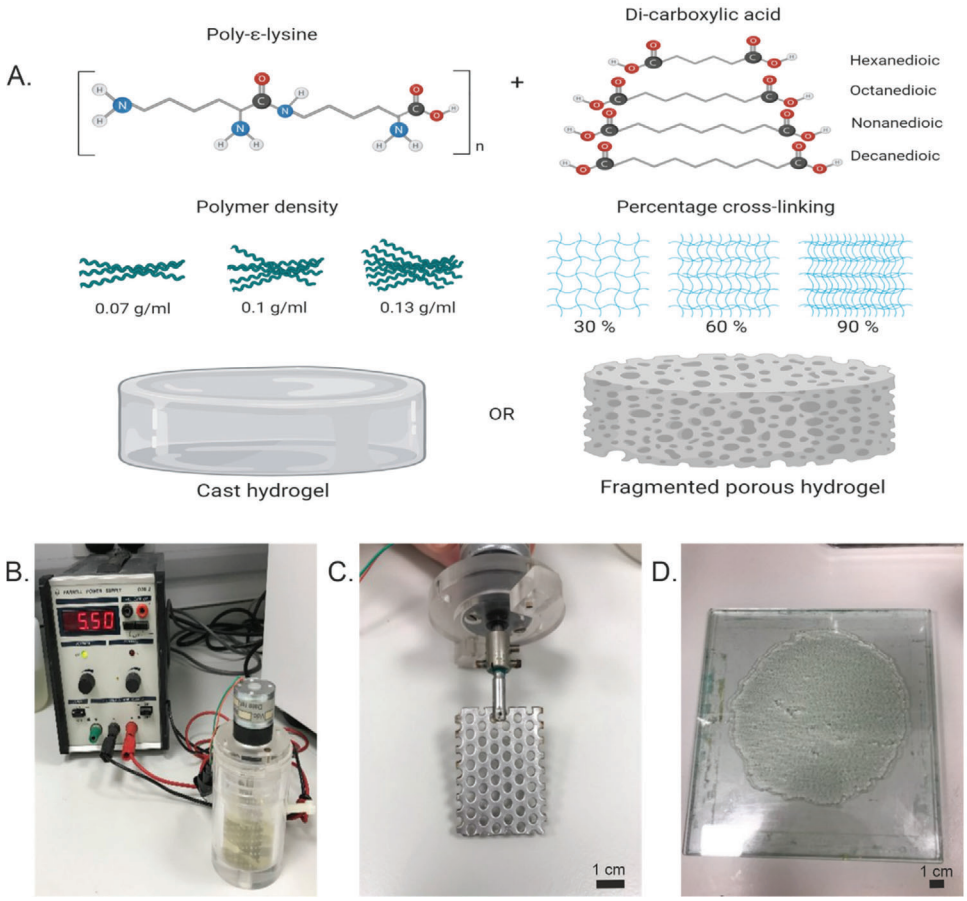

Figure 1. A) Schematic of how to make the variants of the poly-ε-lysine hydrogels; created with BioRender.com. B) Stirrer device used to make fragmented hydrogels. C) Close up of stirrer head used. D) Fragmented hydrogel setting to desired thickness in between glass plates.

Transparency was most affected by the chain length of the bis-carboxylic acid used, increasing the carbon chain length decreased transparency, which was evident across all 60% and 90% pεK hydrogel variants. 60% crosslinked hydrogels ranged between 72.5% ± 14.3 and 97.5% ± 0.6, with the exception of 60-0.07-Dec (55.7% ± 27.8). 60-0.07-Non and 60-0.07-Dec were significantly different to the control, $p < 0.0001$, as were 60-0.1-Dec and 60-0.13-Dec, $p = 0.0109$ and $p = 0.0016$, respectively. When pεK hydrogels were 90% crosslinked, the transparency decreased considerably when the bis-carboxylic acid chain length was >6, this may be due to a higher ratio of bis-carboxylic acid to polymer in the 90% crosslinked hydrogels and hydrophobic interaction between fatty acid chains. 90% Hex-acid (C6) hydrogels had a transmission ≥92% (across the three densities). From the 90% crosslinked hydrogels, Oct-90-0.1 had the second highest light transmission of 74.6% ± 1.9%, however the remaining 90% crosslinked hydrogels were visibly translucent or opaque and would not be suitable for a corneal graft or replacement. They could, however, be considered for tissue engineering applications in the conjunctiva, a membrane that covers the sclera, where transparency is not an essential criterion. All 90% crosslinked variations (90-0.07, 90-0.1, and 90-0.13) in Non-acid and Dec-acid were significantly different to the control $p < 0.0001$, as was 90-0.1-Oct $p = 0.003$. Contact angle analysis revealed that all hydrogels were relatively hydrophilic with contact angles that ranged from 12° to 38° (Figure S2, Supporting Information), and not significantly different to each other, with the exception of only 60-0.1-Dec hydrogel being significantly different to 60-0.1-Hex and 60-0.1-Oct, $p = 0.0064$ and $p = 0.0052$, respectively. These data demonstrate that water easily spread across the surface of the hydrogels, just like tears spread across the surface of the cornea, which is important as it facilitates blinking and clearing of foreign objects and cell debris away from the epithelial surface, maintaining a hydrated cornea and supply of oxygen.[25] The relatively hydrophilic nature of the pεK hydrogels is likely due to the polyamide structure and presence of many charged amine groups on the materials surface. The water content of pεK hydrogels was analyzed by measuring the wet and dry weights (Figure 2D). Hydrogels crosslinked to 60% and 90% follow the same trend with water content decreasing as the density of pεK within the hydrogel increased. With the exception of Non-60-0.13 (55.87% ± 9.86), all other cast pεK hydrogel variants had a water content that ranged from 60.35% ± 0.82 to 81.63% ± 3.74. The only significant differences observed among the hydrogels were 30-0.1-Oct, which was significantly different to 30-0.1-Non, $p = 0.0377$ and 60-0.07-Oct was significantly different to 60-0.13-Oct, $p = 0.0458$. Water in the hydrogel can facilitate oxygen permeability and transport; which may help prevent corneal edema.[26]

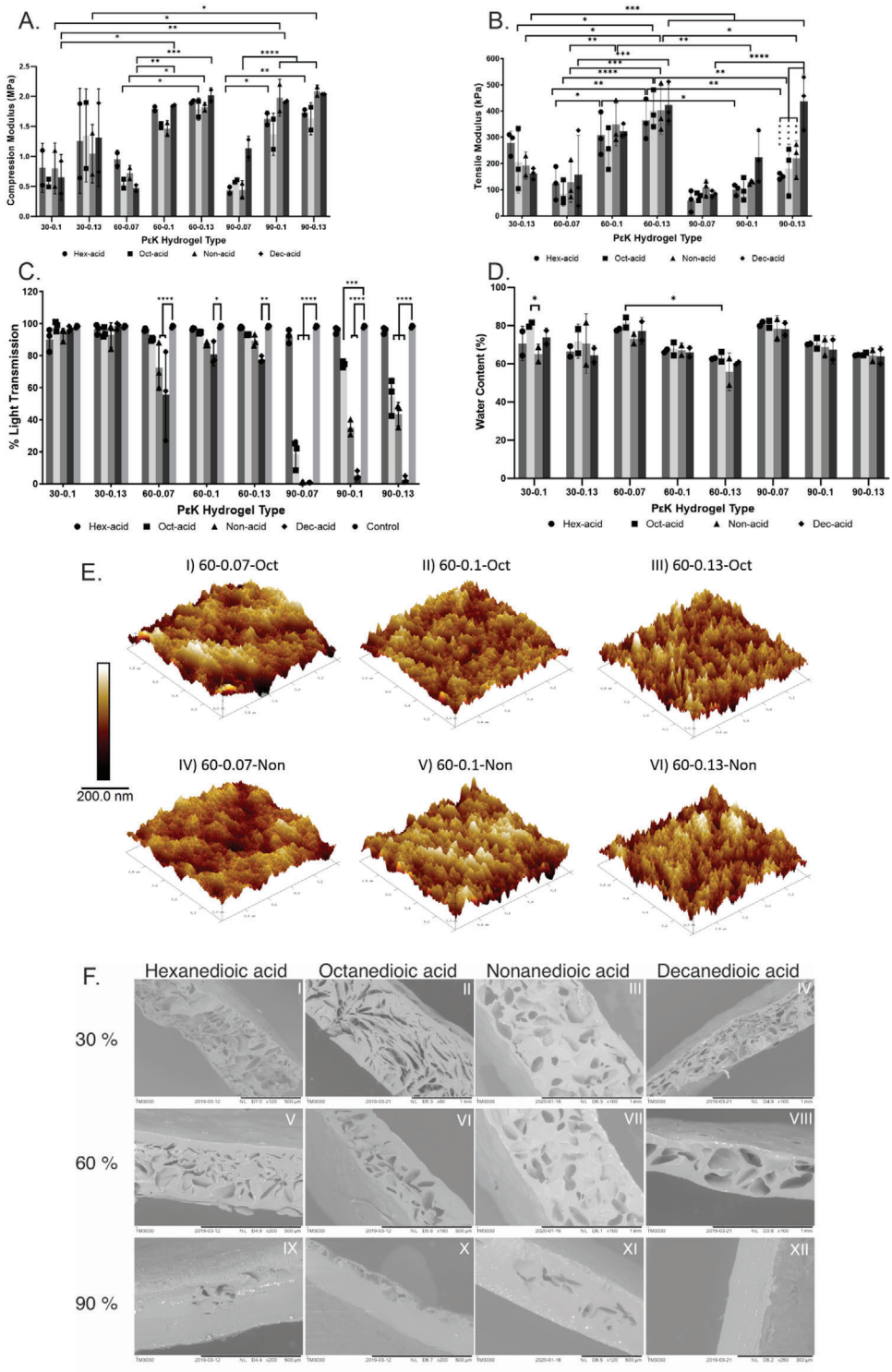

Figure 2. To synthesize hydrogels in (A)–(D), pεK (0.07, 0.1, or 0.13 g cm^{-3}) was crosslinked (30%, 60%, or 90%) with four different biscarboxylic-acids (hexanedioic-acid (Hex), octanedioic-acid (Oct), nonanedioic-acid (Non), and decanedioic-acid (Dec)). The data presented in (A)–(D) represent: A) Average compressive modulus (MPa) of pεK hydrogel variants. 5 samples per run, $n = 2$. B) Average tensile modulus (kPa) of pεK hydrogel variants. 4 samples per run, $n = 3$. C) Average % light transmission at 560 nm of pεK hydrogel variants. 5 samples per run, $n = 3$. D) Average water content (%) of pεK hydrogel variants. 3 samples per run, $n = 2$. E) AFM images demonstrating the topography of pεK hydrogel variants. pεK (0.07, 0.1, or 0.13 g cm^{-3}) was crosslinked 60% with either octanedioic-acid or nonanedioic-acid. Height range 5 to −5 nm. F) SEM images demonstrating the porosity of the cross-sections of pεK hydrogel variants. pεK (0.1 g cm^{-3} was crosslinked (30%, 60%, and 90%) with four biscarboxylic-acids (hexanedioic, octanedioic, nonanedioic, and decanedioic acid). All bars represent averages ±1 standard deviation.

The surface topography of materials is affected by their porosity and roughness, and can influence cell attachment, both Atomic force microscopy (AFM) and scanning electron microscopy (SEM) were used to visualize the hydrogel structure. Surface topography of 60-0.07, 60-0.1, and 60-0.13 Oct-acid and Non-acid pεK hydrogel variants was investigated via AFM (Figure 2E). For AFM analysis, 60% crosslinked hydrogels were chosen as 30% hydrogel variants performed substantially weaker during compression and tensile testing and 90% crosslinked produced hydrogels that were opaque. AFM demonstrated that increasing the density of pεK within the hydrogel changed the nanostructure from a flatter, more open structure (Figure 2E-I,IV) to a closer-knit structure, with slight increased roughness. This was observed in both Oct-acid (Figure 2E-I–III) and Non-acid (Figure 2E-IV–VI) hydrogel types, irrespective of chain length (C8 or C9) of the crosslinker (Oct-acid or Non-acid).

The microstructure of the hydrogel is also dependent upon the chemistry, and can influence the hydrogels mechanical and physical properties. Across all four bis-carboxylic acids, increasing the percentage crosslinking decreased the porosity of the hydrogel, as observed by SEM (Figure 2F). When the bis-carboxylic acid chain length was increased, no obvious differences were seen in the microstructure of the hydrogels. These images advantageously also depict the lack of pores on the surface of the hydrogel. Despite a high porosity being advantageous in the design of tissue engineering constructs, a flat hydrogel surface could be better to support the growth of surface monolayers of cells such as epithelial and endothelial cells present in the cornea. Pores can be introduced into the surface of the hydrogel by an alternative casting method, which establishes an interconnected porosity throughout the hydrogel if required.

In addition to characterization of the cast gel library a preliminary degradation study in an aqueous environment was performed on a smaller selection of 60% crosslinked Oct-acid and Non-acid hydrogel variants, which demonstrated that there was little change in stiffness (Figure S3, Supporting Information) and transparency (Figure S4, Supporting Information) over a 6 month period. No significant differences were observed within the Non-acid hydrogels and only small changes were observed in the Oct-acid variants with 60-0.1-Oct at day 1 being significantly different to 6 month ($p = 0.0309$) and 60-0.13-Oct at day 1 was significantly different to 1 week ($p = 0.0095$). Transparency, with the exception of 60-0.13-Oct at day 1 (80% ± 1.53) across all other hydrogel variants during the 6 months, fell within a similar range of 89% ± 1.32 to 97% ± 1.15 light transmission, demonstrating high transparency throughout the study. Although some statistically significant differences were observed the changes in % light transmission were small. The visual appearance remained transparent and clear. This demonstrates that our hydrogels are hydrolytically biostable and we envisage that any degradation in vivo would be due to cellular enzymes.

Rheological measurements further characterize the mechanical properties of hydrogels. The amplitude sweeps characterize the rigidity of the hydrogels by analyzing the differences in the storage (G') and loss (G'') modulus (**Figure 3**A–C; Table S4A–C, Supporting Information). The crossover point is indicative of the yield point of the hydrogel, where $G' = G''$, demonstrating where the gel switches from "solid-like" to "liquid-like" behavior. Following the crossover point, all of the hydrogel variants rapidly decreased in modulus due to the breakdown of the structure. When the frequency dependence of modulus is evaluated (Figure 3D–F), a higher storage modulus indicates a more "solid-like" behavior, and therefore a stiffer gel, until its yield point. All of the hydrogel variants show parallel G' and G'' throughout the frequency sweep, which further demonstrated typical strong gel behavior. Again, for all four bis-carboxylic acids, the 30% crosslinked hydrogels had the lowest storage modulus, which further indicated these are the least stiff of the gels tested, and are the most susceptible to deformation. When compared to alginate and gelatin hydrogels for tissue engineering applications, the rheological properties were very similar. Several frequency sweep studies of different concentrations of alginate hydrogels yielded G' values of between 2 and 50 kPa,[27] and gelatin hydrogels have a lower storage modulus of 2 kPa.[28] Rheological analysis of porcine corneal tissue demonstrated that the stroma exhibits viscoelastic properties in shear, with shear storage moduli values ranging from 2 to 8 kPa.[29] This shows that poly-ε-lysine had similar elastic properties to two alternative common hydrogels for tissue engineering, and porcine corneal stromal tissue, with all G' values between 1.6 and 3.4 kPa. The complex modulus (G^*) was averaged for the hydrogel variants based on percentage crosslinking and the varying diacid crosslinker (Figure 3G). G^* combines the elastic and viscous contributions and therefore describes the hydrogels entire viscoelastic behavior, characterizing its resistance to deformation. It can be seen that increasing the percentage crosslinking in the hydrogel increases the complex modulus across all four bis-carboxylic acids. This shows understandably that the higher the percentage crosslinking, the more rigid the hydrogel. Significance was seen between the 90-0.1-Dec hydrogels compared to both the 30-0.1-Dec and 60-0.1-Dec variants with p values of 0.0021 and 0.0046, respectively. When analyzing the effect of bis-carboxylic acid crosslinker on the complex modulus, hydrogels crosslinked using nonanedioic acid had the highest complex modulus. This is likely due to the increase in carbon length in the bis-carboxylic acid chain from hexanedioic and octanedioic. The variation in the complex modulus of the 30% and 60% crosslinked decanedioic acid hydrogels may be due to this further increase in carbon chain length, which results in a larger spacing in between the crosslinked pεK, affecting the mechanical properties. It is important to note that as chain length increases, there will be increased hydrophobic interaction between the chains of the crosslinking fatty acid. Significance was seen between the 60-0.1-Non variant and the 60-0.1-Hex and 60-0.1-Dec variants with p values of 0.0368 and 0.0342, respectively. The higher percentage decanedioic acid variant, 90-0.1-Dec also demonstrated significance when compared with 90-0.1-Hex and 90-0.1-Oct with $p = 0.0276$ and 0.0202, respectively.

We have previously shown primary endothelial cell attachment and growth on our cast pεK hydrogels, and demonstrated the presence Na+/K+ATPase, characteristic of a functional endothelial pump mechanism.[18b] Here, we report variations in our pεK hydrogel that can support epithelial cell growth and demonstrate positive ZO-1 expression, characteristic of an epithelial tight junctions and the diffusion barrier mechanism.[30] HCE-T cells were grown on Oct-pεK hydrogel variants in culture for several days to monitor cell attachment and growth across the various hydrogel variants, at a time point were cells had reached

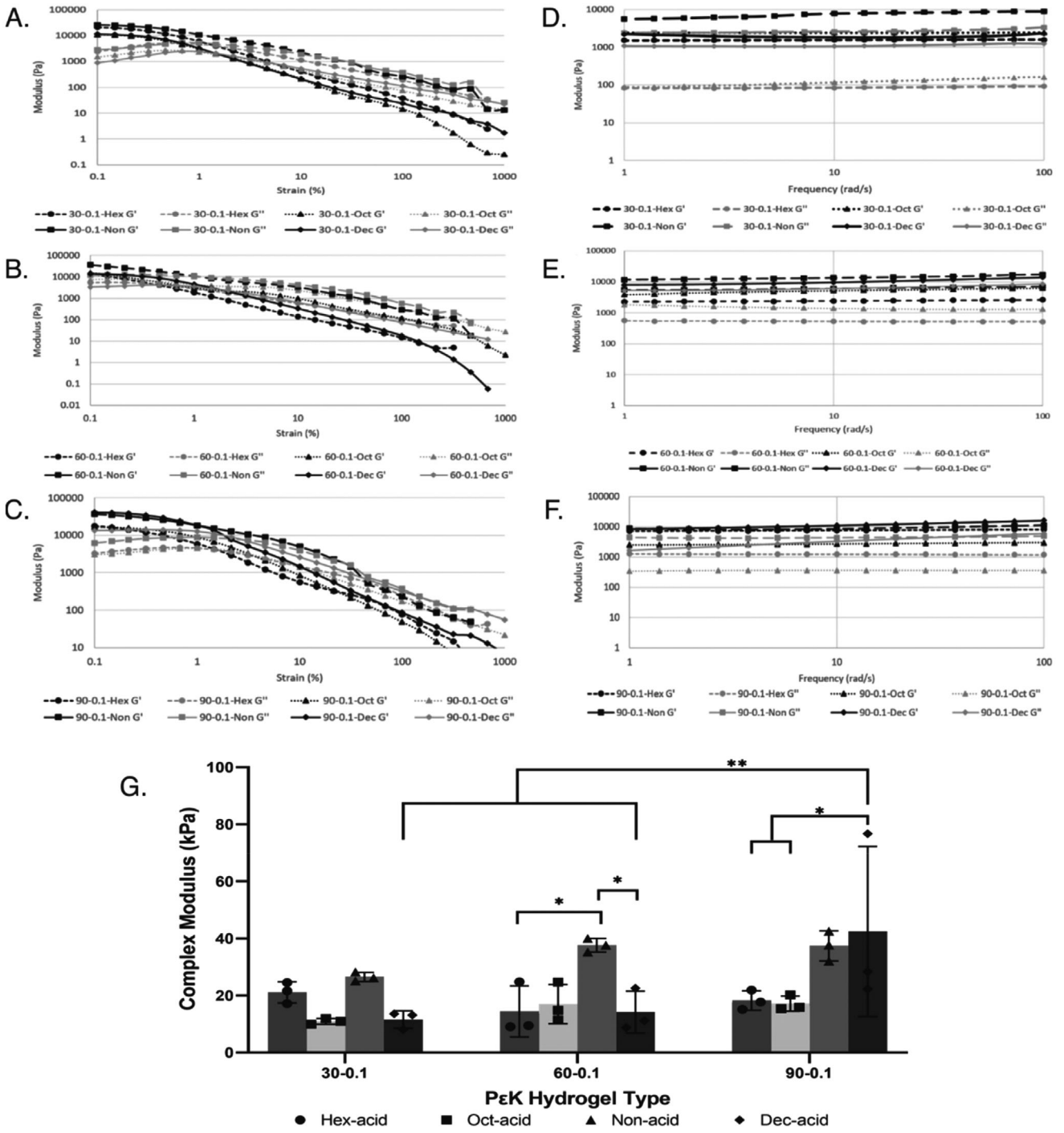

Figure 3. Rheological characterization of cast pεK variants. A–C) Strain sweep: A) 30% crosslinked, B) 60% crosslinked, and C) 90% crosslinked. D–F) Frequency sweep: D) 30% crosslinked, E) 60% crosslinked, and F) 90% crosslinked. G) Complex modulus (G^*) of cast hydrogel variants taken from 0.1% strain from the amplitude sweep.

confluency, 7 days, cells were fixed and immunocytochemical (ICC) staining was performed for the tight junction protein, ZO-1 (**Figure 4**). 30-0.1 was chosen as a representative image for IgG control (Figure S5, Supporting Information). Due to the nature of ICC staining on a hydrogel and a large z-stack image being compiled some background staining was present in all images, however, ZO-1 staining was clearly demonstrated on all Oct-acid hydrogels, with the exception of 90-0.07, which had very little to no positive staining. 60% hydrogel variants established confluent monolayers and positive staining across all

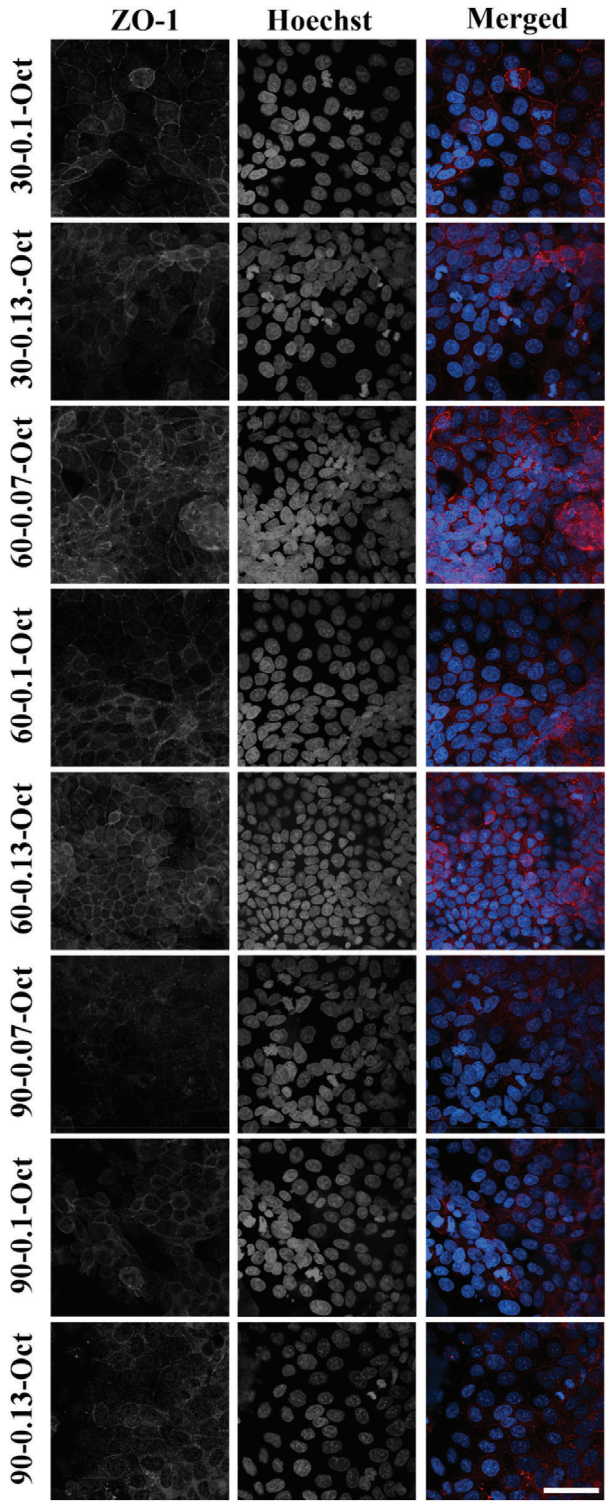

Figure 4. pεK (0.07, 0.1, or 0.13 g mL^{-1}) was crosslinked (30%, 60%, or 90%) with octanedioic-acid (Oct). Micrographs represent HCE-t cells seeded onto Oct hydrogel variants fixed at day 7 and stained for tight junction protein, ZO-1, and nuclei stain, Hoechst 33342. ZO-1 was observed across the pεK hydrogels, however to a lesser extent on the 90% crosslinked variations. All 60% Oct-acid hydrogels demonstrated strong ZO-1 expression for tight junctions and an epithelial monolayer, characteristic of the corneal epithelium. Scale bar represents 50 μm.

density variants localized to the cell wall boundary demonstrating epithelial–epithelial tight junctions were formed on these hydrogel types, an indicative characteristic of epithelial cells.

Particular corneal tissue engineering applications may benefit from a hydrogel with a porosity throughout its full thickness. Porous fragmented hydrogels were created by partial polymerization of the hydrogels under mechanical stirring, and then polymerizing the fragments together in static conditions between two glass plates. Cast gels were created at the same time as controls by static polymerization. The transparency of fragmented pεK hydrogels was analyzed by measuring the % light transmission (**Figure 5**A). Increasing the polymer density reduced the light transmittance, which ranged from 62% ± 11.3 for the highest pεK density (30-0.1-Oct) to 83.6% ± 1.1 for the lowest pεK density (30-0.07-Oct), showing significance between these two extremes, $p = 0.015$. The cast hydrogels with the same polymer chemistry had similar values for light transmittance to each other, ranging from 78% ± 5.5 to 83% ± 1.2; increasing the polymer density has no significant effect on the transparency for these hydrogel variants. The fragmented hydrogels used for cell seeding were 30-0.07-Oct, which had a percentage light transmittance approaching that of the native human cornea at 90%,[31] vital for a corneal application to ensure the restoration of normal vision following implantation. The fragmented hydrogels had a higher water content in comparison to their cast pεK densities equivalents due to water held in interstitial spaces (Figure 5B) with fragmented variants ranging from 92.9% ± 2.1 to 93.2% ± 3.5 and cast variants from 83.3% ± 0.84 to 87.7% ± 1.18 indicative of their porosity, as a higher water content will result from a larger spacing within the hydrogel. Significant differences were observed between 30-0.08-Oct cast and both 30-0.08-Oct fragmented, $p = 0.01$, and 30-0.07-Oct fragmented, $p = 0.008$.

The fragmented porous pεK variants are similar to other polymer hydrogels for corneal tissue engineering and are approaching the mechanical properties of the cornea.[21] Increasing the polymer density increased the compressive modulus for both fragmented and cast hydrogel equivalents (Figure 5C). Fragmenting the hydrogels to introduce pores into the structure reduced the compressive modulus, ranging from 0.037 MPa ± 0.01 to 0.091 MPa ± 0.006 for fragmented variants and from 0.05 MPa ± 0.001 to 0.14 MPa ± 0.1 for cast variants. The 30-0.08-Oct cast hydrogel was significantly stiffer than all other variants, 30-0.07-Oct cast, $p < 0.0001$, 30-0.08-Oct fragmented, $p = 0.001$, and 30-0.07-Oct fragmented, $p < 0.0001$. Further significance was seen between 30-0.08-Oct fragmented and 30-0.07-Oct fragmented, $p = 0.001$ and 30-0.07 cast, $p = 0.004$. Fragmenting the hydrogels is likely to increase the number of fracture points throughout its microstructure, which would allow for cracks to propagate more easily through the structure of the hydrogel and result in failure. The viscoelastic properties of the fragmented and cast pεK hydrogel variants were compared using amplitude and frequency sweeps (Figure 5D–F; Table S5A–C, Supporting Information). In the frequency sweeps, the fragmented and the cast hydrogels performed similarly, with both variants demonstrating stable "gel-like" behavior. The cast hydrogels showed similar or higher storage moduli at 10 rad s^{-1} than the fragmented hydrogels, demonstrating a higher resistance to deformation. The differences were significant in the storage moduli at 10 rad s^{-1}, between 30-0.08-Oct cast with 30-0.07-Oct cast,

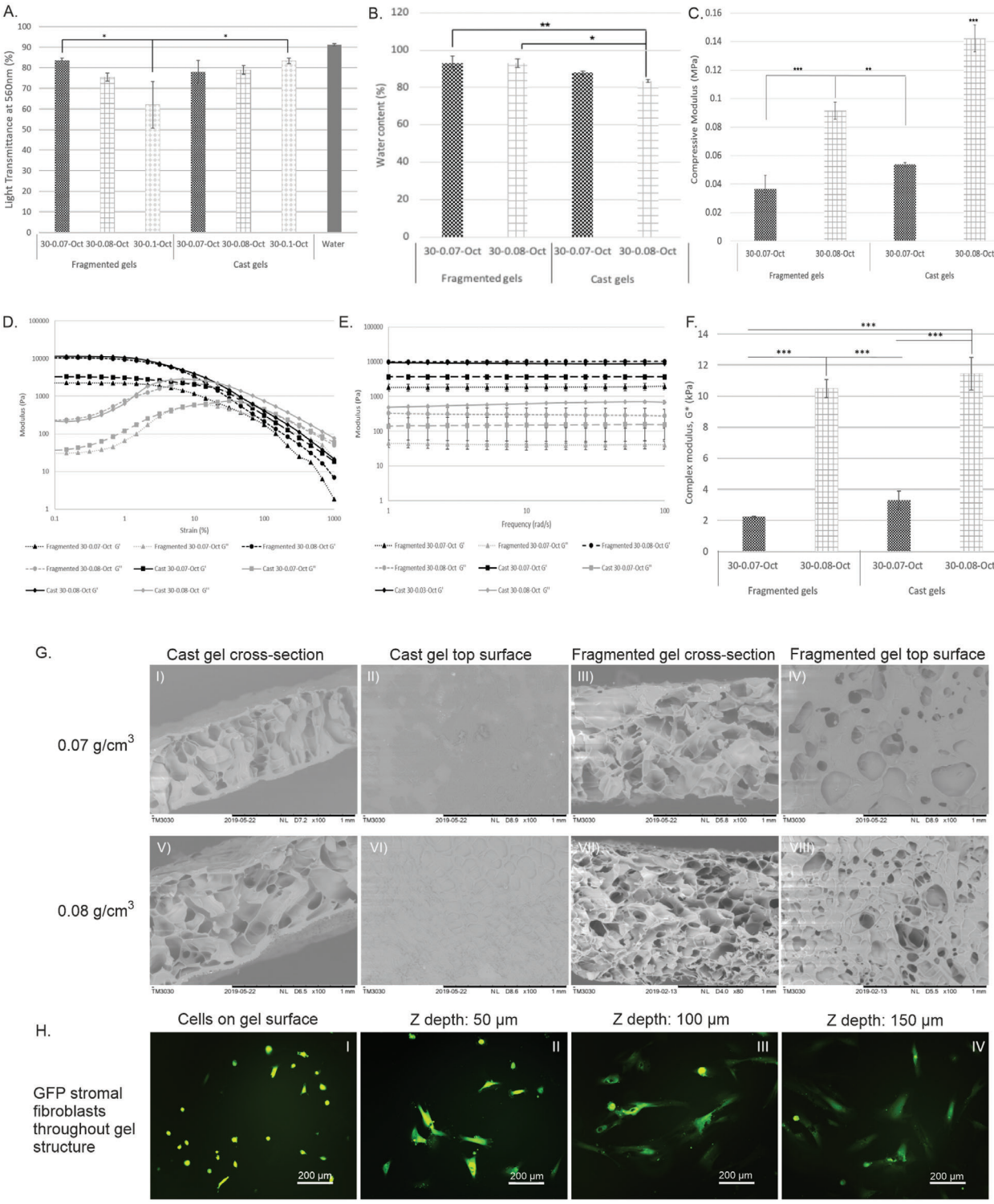

Figure 5. pεK hydrogels (pεK density of 0.07, 0.08, or 0.1 g cm^{-3}), crosslinked 30% with octanedioic acid, were prepared by polymerization under mechanical stirring to fragment or by static casting. A) Bar chart representing average light transmittance (%) of pεK hydrogel variants. 5 samples per run, $n = 3$. B) Bar chart representing average water content (%) of pεK hydrogel variants. 3 samples per run, $n = 3$. C) Bar chart representing compressive modulus of pεK hydrogel variants. 5 samples per run, $n = 3$. D) Line chart representing the storage and loss modulus of pεK hydrogel variants over an amplitude sweep. $n = 3$. E) Line chart representing the storage and loss modulus of pεK hydrogel variants over a frequency sweep, $n = 2$. F) Bar chart representing the complex modulus (G^*) of the fragmented and cast hydrogel variants taken from the amplitude sweep. $n = 3$. G) SEM images demonstrating the porosity of cast and fragmented pεK hydrogel variants. H) Fluorescent micrographs of GFP human stromal fibroblasts grown on 30-0.07-Oct fragmented hydrogels at day 21. Imaged using a Nikon Ti-E fluorescent microscope. Scale bars equal 200 µm.

$p = 0.002$ and 30-0.07-Oct fragmented, $p = 0.001$, and between 30-0.08-Oct fragmented with 30-0.07-Oct cast and 30-0.07-Oct fragmented, with $p = 0.001$ and $p = 0.0003$, respectively. There were no significant differences observed in the loss moduli of the fragmented and cast hydrogel variants. Again, the complex moduli was calculated for the different hydrogel variants to determine the resistance of the hydrogel to deformation. It can be seen that increasing the polymer density has the biggest influence on the complex modulus, with both the fragmented and cast 0.08 g cm^{-3} variants being significantly higher than the lower 0.07 g cm^{-3} variants, all p values <0.001. Fragmenting the hydrogels reduced the complex modulus of the hydrogels when compared with cast variants, however, this had less of an influence.

An interconnected porosity is important for a tissue engineering scaffold to allow for the infiltration and migration of cells into the construct. SEM analysis was used to investigate the porosity of both fragmented and cast 30-0.07-Oct and 30-0.08-Oct pεK hydrogels. The fragmented hydrogel micrographs demonstrated an interconnected porosity throughout both the cross-section and top surface, whereas the cast hydrogels had no pores on the surface (Figure 5G). A pore size of 20 µm has been reported as a minimum to facilitate the integration of corneal stromal cells and allow for an adequate surface area for cell adhesion.[32] When GFP-transduced stromal fibroblasts were seeded into the fragmented hydrogels, 30-0.07-Oct, for 21 days they migrated into its porous structure (Figure 5H). The cells were initially seeded on top of the porous hydrogel, and had a rounded morphology, however over time, the cells migrated down into the network and began to demonstrate their fibroblastic phenotype. Human corneal fibroblasts (hCFs) were observed at different z depths throughout the hydrogel using a volume plot and color coding, up to a depth of 650 µm (Figure S6, Supporting Information). The ingrowth of cells into the porous hydrogel and their distribution throughout the scaffold could facilitate important cell functions such as ECM production and cellular communication with the epithelial and endothelial layers.[33] The migration of the stromal fibroblasts through the porous fragmented pεK hydrogel and maintenance of cell growth gives confidence of cytocompatibility.

The use of a synthetic corneal replacement could be beneficial to overcome the shortage and variability in donor tissue, in addition to the limitations in host response and cell integration. Here and previously, we demonstrate the integration of epithelial, endothelial, and stroma cells on and within of pεK hydrogels.[18b] The combination of incorporating these specific cells together with the added antimicrobial benefits of our pεK hydrogels could prove advantageous to the corneal tissue engineering field.[16,17,18a,34]

3. Conclusion

In summary, a library of hydrogel materials based on pεK has been developed by varying the bis-carboxylic acid crosslinker, the percentage crosslinking and the polymer density. These hydrogels have been characterized to assess their suitability for corneal tissue engineering applications. They can be manufactured in order to produce either porous or nonporous sheets, which both demonstrated a high transparency, water content, and tunable mechanical properties. The cast sheets were able to support the adherence and growth of a corneal epithelial monolayer and demonstrated tight junction staining, and the fragmented hydrogels encouraged the migration of stromal fibroblasts into the porous network. Both of these elements are crucial considerations for a successful corneal tissue replacement. This study has demonstrated the versatile nature of pεK hydrogels, and presents it as a potential candidate biomaterial for corneal regeneration.

Supporting Information

Supporting Information is available from the Wiley Online Library or from the author.

Acknowledgements

R.L. and G.L.D. contributed equally to this work. This work was funded by EPSRC grant no. EP/M002209/1 and an EPSRC DTA studentship for G.D. The authors are grateful to the School of Engineering (University of Liverpool) for access to the AFM and the rheometer, and to Dr. Tim Joyce and Dr. Riaz Akhtar and Prof. Rob Poole for providing technical assistance. The authors would also like to acknowledge Danielle O'Loughlin for assistance with primary stromal cell extraction and culture.

Conflict of Interest

The authors declare no conflict of interest.

Data Availability Statement

The data for this work can be found at http://doi.org/10.17638/datacat.liverpool.ac.uk/1213.[35]

Keywords

characterization, cornea, hydrogel, ocular surface, poly-lysine

Received: January 28, 2021
Revised: March 23, 2021
Published online:

[1] D. W. Delmonte, T. Kim, *J. Cataract Refractive Surg.* **2011**, *37*, 588.
[2] R. Williams, R. Lace, S. Kennedy, K. Doherty, H. Levis, *Adv. Healthcare Mater.* **2018**, *7*, 1701328.
[3] S. Matthyssen, B. Van Den Bogerd, S. N. Dhubhghaill, C. Koppen, N. Zakaria, *Acta Biomater.* **2018**, *69*, 31.
[4] I. Brunette, C. J. Roberts, F. Vidal, M. Harissi-Dagher, J. Lachaine, H. Sheardown, G. M. Durr, S. Proulx, M. Griffith, *Prog. Retinal Eye Res.* **2017**, *59*, 97.
[5] R. Lace, C. Murray-Dunning, R. Williams, *J. Mater. Sci.* **2015**, *50*, 1523.
[6] a) L. J. Bray, K. A. George, S. L. Ainscough, D. W. Hutmacher, T. V. Chirila, D. G. Harkin, *Biomaterials* **2011**, *32*, 5086; b) L. Guan, P. Tian, H. Ge, X. Tang, H. Zhang, L. Du, P. Liu, *J. Mol. Histol.* **2013**, *44*, 609.
[7] I. Ortega, R. Mckean, A. J. Ryan, S. Macneil, F. Claeyssens, *Biomater. Sci.* **2014**, *2*, 723.
[8] a) P. Fagerholm, N. S. Lagali, K. Merrett, W. B. Jackson, R. Munger, Y. Liu, J. W. Polarek, M. Soderqvist, M. Griffith, *Sci. Transl. Med.* **2010**, *2*, 46ra61; b) A. Shalaby Bardan, N. Al Raqqad, M. Zarei-Ghanavati, C. Liu, *Eye* **2018**, *32*, 7.

[9] M. Griffith, D. G. Harkin, *Curr. Opin. Ophthalmol.* **2014**, *25*, 240.
[10] a) Y. Wang, W. Zhang, C. Gong, B. Liu, Y. Li, L. Wang, Z. Su, G. Wei, *Soft Matter* **2020**, *16*, 10029; b) F. Gelain, Z. Luo, M. Rioult, S. Zhang, *npj Regener. Med.* **2021**, *6*, 9; c) M. Sinha, T. Gupte, *Int. Ophthalmol.* **2018**, *38*, 1225.
[11] D. Myung, P.-E. Duhamel, J. R. Cochran, J. Noolandi, C. N. Ta, C. W. Frank, *Biotechnol. Prog.* **2008**, *24*, 735.
[12] E. C. Wu, S. Zhang, C. A. E. Hauser, *Adv. Funct. Mater.* **2012**, *22*, 456.
[13] L. Wang, C. Gong, X. Yuan, G. Wei, *Nanomaterials* **2019**, *9*, 285.
[14] S. Mondal, S. Das, A. K. Nandi, *Soft Matter* **2020**, *16*, 1404.
[15] A. Jain, L. Sailaja Duvvuri, S. Farah, N. Beyth, A. J. Domb, W. Khan, *Adv. Healthcare Mater.* **2014**, *3*, 1969.
[16] A. G. Gallagher, J. A. Alorabi, D. A. Wellings, R. Lace, M. J. Horsburgh, R. L. Williams, *Adv. Healthcare Mater.* **2016**, *5*, 2013.
[17] a) S. M. Kennedy, P. Deshpande, A. G. Gallagher, M. J. Horsburgh, H. E. Allison, S. B. Kaye, D. A. Wellings, R. L. Williams, *Invest. Ophthalmol. Visual Sci.* **2020**, *61*, 18; b) R. Lace, K. G. Doherty, D. Dutta, M. D. P. Willcox, R. L. Williams, *Adv. Mater. Interfaces* **2020**, *7*, 2001232.
[18] a) A. G. Gallagher, K. McLean, R. M. K. Stewart, D. A. Wellings, H. E. Allison, R. L. Williams, *Invest. Ophthalmol. Visual Sci.* **2017**, *58*, 4499; b) S. Kennedy, R. Lace, C. Carserides, A. G. Gallagher, D. A. Wellings, R. L. Williams, H. J. Levis, *J. Mater. Sci.: Mater. Med.* **2019**, *30*, 102.
[19] D. A. Wellings, (Spheritech Ltd.) 9938378, **2018**.
[20] R. N. Palchesko, S. D. Carrasquilla, A. W. Feinberg, *Adv. Healthcare Mater.* **2018**, *7*, 1701434.
[21] D. C. Pye, *PLoS One* **2020**, *15*, e0224824.
[22] E. Kim, M. Saha, K. Ehrmann, *Eye Contact Lens* **2018**, *44*, S148.
[23] C. Vepari, D. L. Kaplan, *Prog. Polym. Sci.* **2007**, *32*, 991.
[24] W. L. Stoppel, C. E. Ghezzi, S. L. Mcnamara, L. D. Black III, D. L. Kaplan, *Ann. Biomed. Eng.* **2015**, *43*, 657.
[25] I. K. Reddy, W. Aziz, R. B. Sause, in *Ocular Theraputics and Drug Delivery* (Ed: I. K. Reddy), CRC Press, Boca Raton, FL **1995**, p. 171.
[26] C. S. A. Musgrave, F. Fang, *Materials* **2019**, *12*, 261.
[27] a) N. K. Pengfei Duan, J. Wang, J. Chen, *Biomater. Soft Mater.* **2017**, *2*, 1309; b) J. Hilbig, K. Hartlieb, M. Gibis, K. Herrmann, J. Weiss, *Food Hydrocolloids* **2020**, *101*, 105487.
[28] H. Goodarzi, K. Jadidi, S. Pourmotabed, E. Sharifi, H. Aghamollaei, *Int. J. Biol. Macromol.* **2019**, *126*, 620.
[29] H. Hatami-Marbini, *J. Biomech.* **2014**, *47*, 723.
[30] a) J. Anderson, M. Balda, A. Fanning, *Curr. Opin. Cell Biol.* **1993**, *5*, 772; b) J.-A. Ko, Y. Liu, R. Yanai, T.-i. Chikama, T. Takezawa, T. Nishida, *Invest. Ophthalmol. Visual Sci.* **2008**, *49*, 113.
[31] a) E. M. Beems, J. A. Van Best, *Exp. Eye Res.* **1990**, *50*, 393; b) K. M. Meek, C. Knupp, *Prog. Retinal Eye Res.* **2015**, *49*, 1.
[32] R. Parke-Houben, C. H. Fox, L. L. Zheng, D. J. Waters, J. R. Cochran, C. N. Ta, C. W. Frank, *J. Mater. Sci.: Mater. Med.* **2015**, *26*, 107.
[33] C. Fan, D.-A. N. Wang, *Tissue Eng., Part B* **2017**, *23*, 451.
[34] J. Aveyard, R. C. Deller, R. Lace, R. L. Williams, S. B. Kaye, K. N. Kolegraff, J. M. Curran, R. A. D'Sa, *ACS Appl. Mater. Interfaces* **2019**, *11*, 37491.
[35] R. Doherty, G. Duffy, K. Doherty, R. Williams, Liverpool Data Catalogue, **2021**, https://doi.org/10.17638/datacat.liverpool.ac.uk/1213.